Available online at www.sciencedirect.com
ScienceDirect
European Journal of Mechanics B/Fluids 27 (2008) 24–41

The effect of a depth-dependent bubble distribution on the normal modes of internal waves: quasistatic approximation

R.H.J. Grimshaw [a], K.R. Khusnutdinova [a,*], L.A. Ostrovsky [b]

[a] *Department of Mathematical Sciences, Loughborough University, Loughborough LE11 3TU, UK*
[b] *Zel Technologies/University of Colorado, R/ET-O, 325 Broadway, Boulder, CO 80305, USA*

Received 14 December 2006; received in revised form 23 February 2007; accepted 6 March 2007

Available online 21 March 2007

Abstract

We consider internal and surface waves propagating horizontally in the fluid waveguide, formed by an underlying density stratification. As well as the usual basic density stratification, we are concerned with the effect of a nearly stationary depth-dependent distribution of bubbles. While our previous work was restricted to the case of a locally monodisperse mixture, in this paper we show that by using a quasistatic approximation (where attention is confined to those modes whose typical frequencies are much less than the natural frequency for bubble oscillations), we can extend that work to the case of more general discrete and continuous bubble distributions. The equations of motion are formulated in terms of the usual fluid variables and the void fraction of bubbles. Then, to leading order in the Boussinesq approximation, we obtain the usual equation for internal wave modes, but the value of the buoyancy frequency in the fluid is replaced by an effective buoyancy frequency which takes account of the bubble distribution. Indeed, in some circumstances the bubble distribution could be entirely responsible for the density stratification, and hence can give rise to its own internal wave field. Two physical factors are shown to affect the buoyancy frequency in the mixture: the effective stratification due to the bubbles adds to the effect of stratification in the liquid, while the compressibility of the mixture due to the bubbles reduces the buoyancy frequency. Having in mind possible applications of our model to oceanic situations and in accordance with existing observational evidence that the void fraction profile in the ocean decays exponentially with depth, we obtain an explicit description of the normal modes for several simple models of the basic density profile and show that bubble distributions, when present, may considerably change the properties of the internal waveguide.

PACS: 47.55.Hd; 47.55.Kf

Keywords: Normal modes; Bubbles; Internal waves

1. Introduction

Horizontally propagating internal waves arise in fluids where there is a basic depth-dependent density profile, and have been intensively studied, often in an oceanic context. Our concern here is with the effect on the internal and

* Corresponding author. Tel.: +44 (0)1509 228202; fax: +44 (0)1509 223969.
E-mail addresses: R.H.J.Grimshaw@lboro.ac.uk (R.H.J. Grimshaw), K.Khusnutdinova@lboro.ac.uk (K.R. Khusnutdinova), Lev.A.Ostrovsky@noaa.gov (L.A. Ostrovsky).

0997-7546/$ – see front matter
doi:10.1016/j.euromechflu.2007.03.002

surface waves in this waveguide when there is, in addition, a depth-dependent distribution of bubbles. Such a situation is certainly conceptually feasible, and, indeed, such distributions of bubbles may arise in many fluid situations of practical interest (e.g., in the upper layer of the ocean, which is our main concern here, or in technological processes using aerated fluids, such as deep-water oil drilling).

Previously (Grimshaw and Khusnutdinova [1,2]) we have used a two-dimensional model of a dilute locally monodisperse mixture of an incompressible fluid with gas bubbles to model and study internal waves in the presence of a depth-dependent distribution of bubbles. Here, this work is extended to more realistic polydisperse mixtures, when, at each fixed depth, there is either a discrete or a continuous distribution of bubbles. We restrict our attention to the low-frequency situation, where we assume that the characteristic frequencies of the normal modes are much less than the natural frequency for bubble oscillations. This assumption leads to a *quasistatic* approximation for the interaction of the bubbles with the fluid, in which only a pressure balance is needed and the high-frequency radial oscillations of the bubbles are ignored. In this approximation, we can formulate the mathematical model in terms of the usual fluid variables, and only the total void fraction of bubbles, thus allowing us to consider more general bubble distributions. We then use a form of the Boussinesq approximation, to obtain an explicit analytical description of the normal modes (including the surface wave mode) for the important case of a near-surface (exponentially decaying with depth) void fraction. Our results show that bubble distributions, when present, can have a profound effect on the structure of the internal wave field (but do not significantly affect the surface wave mode). As we show in Section 4, bubbles can support their own "bubble" modes of internal waves, even in an otherwise homogeneous fluid. If there is a background density stratification which is present in the absence of any bubbles, supporting one or more internal modes, then the weak coupling introduced through the interaction of the two waveguides induces a splitting of the dispersion curves, which is reflected in the behaviour of the respective modal functions. In the simple case when the background density stratification (in the absence of bubbles) is modelled by a two-layer fluid, so that there is just a single pycnocline mode, the splitting of the dispersion curves is most pronounced for a shallow pycnocline, and a relatively large void fraction for the bubbles compared to the density jump across the interface. Otherwise, for a deeper pycnocline, or for a larger density jump across the pycnocline, or for a smaller void fractions of bubbles, the splitting of the dispersion curves is still present, but is less pronounced, resulting in a pycnocline mode which has a similar structure to the bubble modes. Finally, if the pycnocline is well separated from the bubble layer, then there is virtually no interaction between the pycnocline mode and the bubble modes, and we have two independent waveguides located at different depths.

Although our present model may be applicable in various situations, in this paper we have focused on possible oceanic applications. The internal wave field constitutes a fundamental component of the ocean. For sufficiently large horizontal scales, it is customary to take account of the ocean's free surface and rigid bottom, and so reduce the study of internal waves to a normal mode structure with associated horizontal propagation features (e.g., LeBlond and Mysak [3], Gill [4], Miropol'sky [5]). It is well known that breaking surface waves inject bubbles into the ocean surface layer. Since density variations in the ocean are usually small, typical void fractions of bubbles in the upper ocean may significantly change the density gradient field. Until recently, this feature has not been taken into account in determining the structure of normal modes. However, developments both in the observations of the structure of the bubble layer in the upper ocean (e.g., Thorpe [6], Farmer, Vagle and Li [7], Terrill and Melville [8]), and in the mechanics of multiphase media (e.g., Nigmatulin [9]), have allowed us to begin the consideration of the effect of bubbles on normal modes (Grimshaw and Khusnutdinova [1,2]).

According to Thorpe [6], for winds exceeding 6.5 $\mathrm{m\,s^{-1}}$ there is a continuous bubble layer of variable thickness in the upper ocean, which may extend to a depth of several meters beneath the surface (see Farmer and Vagle [10], Zedel and Farmer [11], and Farmer et al. [7]). The observed bubble layer is highly structured, varies both spatially and temporally, and depends significantly on the wind speed. In general, there is a monotonic decrease in the bubble void fraction with increasing depth; the void fraction profile either decays exponentially, or may follow an inverse-square profile (Buckingham [12]). According to Farmer and Lemon [13], the bubble concentration decreases exponentially with depth, with an e-folding scale of order 1 m, which depends on the wind speed. The number density of bubbles as a function of the bubble radius has a peak at all depths, and decreases rapidly on either side of the peak, and also rapidly with depth (see, e.g., Thorpe [14], Farmer et al. [7], Terrill and Melville [8] and the references there). These observations have shown that bubbles with radii of approximately 50–100 μm contribute most to the total void fraction (Farmer et al. [7]). A fuller review of the data gathered on the distributions of bubbles in the ocean can be found in our earlier work (Grimshaw and Khusnutdinova [1,2]).

2. Model formulation

We consider a polydisperse mixture of an inviscid, incompressible fluid with small gas bubbles, which is bounded above by a free surface and below by a flat rigid boundary. We suppose that the flow is two-dimensional, and use the spatial coordinates (x, z) where x is horizontal and z is vertical. The rigid bottom is at $z = -H$ and the undisturbed free surface is at $z = 0$.

We follow an approach developed in the mechanics of multiphase media (e.g., Nigmatulin [9]). The bubbles are assumed to preserve their mass and spherical form. The distances between the bubbles are supposed to be large enough to prevent collisions, and so the interaction between the bubbles is due only to pressure changes. The processes of bubble formation and destruction are not taken into account, and it is assumed that the bubbles, on average, move with the velocity of the fluid flow. The fluid phase is assumed to be incompressible, following the traditional approach towards studying internal waves (in the absence of bubbles). This is also justified by the great compressibility of bubbles compared to that of the surrounding fluid, and their small physical dimensions. The void fraction α_g is supposed to be small enough, $\alpha_g \ll 1$, so that the mass of the gas is neglected compared to the mass of the fluid. Thus, the mixture can be considered as a medium with density ρ approximately equal to $\rho_l(1-\alpha_g)$ where ρ_l is the density field of the fluid phase. Here, surface tension and dissipative mechanisms are not taken into account (for a discussion of these effects see Grimshaw and Khusnutdinova [1,2]).

Under these assumptions the set of equations describing two-dimensional motion of the mixture takes the form

$$\rho\frac{\mathrm{d}u}{\mathrm{d}t} + p_x = 0, \qquad \rho\frac{\mathrm{d}w}{\mathrm{d}t} + p_z + \rho g = 0, \tag{1}$$

$$\frac{\mathrm{d}\rho}{\mathrm{d}t} + \rho(u_x + w_z) = 0, \qquad \frac{\mathrm{d}n_i}{\mathrm{d}t} + n_i(u_x + w_z) = 0, \tag{2}$$

$$\rho_l\left(R_i\frac{\mathrm{d}^2R_i}{\mathrm{d}t^2} + \frac{3}{2}\left(\frac{\mathrm{d}R_i}{\mathrm{d}t}\right)^2\right) = p_{gi} - p, \tag{3}$$

$$\frac{\mathrm{d}\rho_l}{\mathrm{d}t} = 0, \qquad \rho = \rho_l(1-\alpha_g), \qquad \alpha_g = \frac{4}{3}\pi\sum_{i=1}^{N} n_i R_i^3, \tag{4}$$

$$\frac{\mathrm{d}}{\mathrm{d}t}\left(p_{gi}R_i^{3\kappa}\right) = 0. \tag{5}$$

Here p, ρ, u, w are pressure, density and velocity components of the mixture; ρ_l is the density of a pure fluid; p_{gi}, R_i, n_i are pressure, radius and number density of bubbles of the ith fraction ($i = 1, 2, \ldots, N$, fractions are characterised by the size of bubbles in the basic state); α_g is the total void fraction; κ is a polytropic exponent of a gas ($1 \leqslant \kappa \leqslant \gamma_g$, where γ_g is the adiabatic exponent of a gas) and

$$\frac{\mathrm{d}}{\mathrm{d}t} = \frac{\partial}{\partial t} + u\frac{\partial}{\partial x} + w\frac{\partial}{\partial z}$$

is the material derivative with respect to time. In this model, the basic fluid equations for the mixture are closed by the Rayleigh equation (3) for the bubble oscillations (Rayleigh [15]), where the pressure at infinity is replaced by the pressure of the mixture. Eq. (5) follows from the conservation laws

$$\frac{\mathrm{d}}{\mathrm{d}t}\left(\ln p_{gi}\rho_{gi}^{-\kappa}\right) = 0 \quad \text{and} \quad \frac{\mathrm{d}}{\mathrm{d}t}\left(\rho_{gi}R_i^3\right) = 0,$$

where ρ_{gi} is the density of the gas (for bubbles of the ith fraction). Here, the first law generalises conservation laws for temperature ($\kappa = 1$) and entropy ($\kappa = \gamma_g$) of the gas and is similar to the polytropic law. The second law follows from conservation of the mass of a spherical bubble. This is essentially the Iordansky [16], Kogarko [17], Wijngaarden [18] model, modified to take gravity, and the depth-dependence of the void fraction, into account (see also Nigmatulin [9]). For a fuller discussion of the model in the monodisperse case see Grimshaw and Khusnutdinova [1,2].

Here, we consider in more detail the low-frequency situation, when the characteristic frequency of a wave is small compared to the natural frequency of bubble oscillations also known as Minnaert frequency (Minnaert [19]):

$$\omega \ll \omega_* = \sqrt{\frac{3\kappa p_*}{R_*^2\rho_*}},$$

where p_* and ρ_* are the local pressure and density of the mixture, and R_* is the radius of a bubble. For example, for typical oceanic conditions $R_* \approx 50$–100 μm, $p_* \approx 10^5$ Pa, $\rho_* \approx 10^3$ kg m^{-3}, $\kappa = 1.4$, which leads to $\omega_* \approx (2\text{–}4) \times 10^5$ s^{-1}. Thus, this assumption is appropriate when studying internal waves. In this case, we may neglect the left-hand side of the Rayleigh equation (3), as these terms are responsible for high-frequency bubble oscillations. This approximation yields

$$p_{gi} = p, \quad \text{for all } i.$$

This is called the *quasistatic* approximation, (e.g., Naugolnykh and Ostrovsky [20]). Then, from (5), we obtain

$$\frac{\mathrm{d}}{\mathrm{d}t} \ln\left(p^{1/\kappa} R_i^3\right) = 0, \quad \text{for all } i. \tag{6}$$

From (2) we have

$$\frac{\mathrm{d}}{\mathrm{d}t} \ln(n_i) = -(u_x + w_z), \quad \text{for all } i. \tag{7}$$

Adding Eqs. (6) and (7) with a subsequent summation over all values of i yields

$$\frac{\mathrm{d}}{\mathrm{d}t}\left(p^{1/\kappa}\alpha_g\right) + p^{1/\kappa}\alpha_g(u_x + w_z) = 0. \tag{8}$$

From the second equation in (4) we find that

$$\frac{\mathrm{d}\rho}{\mathrm{d}t} = -\rho_l \frac{\mathrm{d}\alpha_g}{\mathrm{d}t} = -\frac{\rho}{1-\alpha_g}\frac{\mathrm{d}\alpha_g}{\mathrm{d}t}.$$

Therefore, we can exclude ρ_l from all equations. As a result, in the quasistatic approximation, we have the following reduced system of equations for the variables ρ, p, u, w, α_g:

$$\rho\frac{\mathrm{d}u}{\mathrm{d}t} + p_x = 0, \qquad \rho\frac{\mathrm{d}w}{\mathrm{d}t} + p_z + \rho g = 0, \tag{9}$$

$$\frac{1}{\rho}\frac{\mathrm{d}\rho}{\mathrm{d}t} = -\frac{1}{1-\alpha_g}\frac{\mathrm{d}\alpha_g}{\mathrm{d}t}, \qquad u_x + w_z = \frac{1}{1-\alpha_g}\frac{\mathrm{d}\alpha_g}{\mathrm{d}t}, \tag{10}$$

$$\frac{\mathrm{d}}{\mathrm{d}t}\left(p^{1/\kappa}\alpha_g\right) + p^{1/\kappa}\alpha_g(u_x + w_z) = 0. \tag{11}$$

This equation set has the same form as that for a monodisperse mixture in this present quasistatic approximation.

It is useful to note that this reduced equation set can also be obtained from a continuous distribution of bubbles, which may be a more realistic representation of oceanic bubble distributions. This case can be viewed as the limit when the number of bubble fractions becomes infinitely large. In this case, we assume that the bubbles are distributed by their size in the basic state, and $c(R_0, z)\,\mathrm{d}R_0$ is the number density of bubbles with radii in the interval from R_0 to $R_0 + \mathrm{d}R_0$. Then, the void fraction of bubbles in the basic state is

$$\alpha_{g0}(z) = \int_{R_{0\min}}^{R_{0\max}} \frac{4}{3}\pi R_0^3 c(R_0, z)\,\mathrm{d}R_0.$$

In the perturbed state, we define the void fraction as

$$\alpha_g = \int_{R_{0\min}}^{R_{0\max}} \frac{4}{3}\pi R(R_0, t, x, z)^3 c(R_0, t, x, z)\,\mathrm{d}R_0.$$

The case for a finite number of bubble fractions is recovered by setting

$$c(R_0, t, x, z) = \sum_{i=1}^{N} n_i(t, x, z)\delta(R_0 - a_i), \quad i = 1, 2, \ldots, N.$$

Next we require that the number of bubbles, which in the basic state have radii in the interval from R_0 to $R_0 + \mathrm{d}R_0$, is preserved,

$$\frac{\mathrm{d}c}{\mathrm{d}t} + c(u_x + w_z) = 0. \tag{12}$$

The perturbed radius R should satisfy the Rayleigh equation. But, again, we restrict our attention to the low-frequency quasistatic limit, so that locally, $p_g = p$, and hence

$$\frac{\mathrm{d}}{\mathrm{d}t}\left(p^{1/\kappa} R^3\right) = 0. \tag{13}$$

Multiplying (13) by $\frac{4}{3}\pi c(R_0, t, x, z)$ and integrating with respect to R_0, we obtain

$$\frac{\mathrm{d}}{\mathrm{d}t}\left(p^{1/\kappa} \int_{R_{0\min}}^{R_{0\max}} \frac{4}{3}\pi R^3 c \,\mathrm{d}R_0\right) - p^{1/\kappa} \int_{R_{0\min}}^{R_{0\max}} \frac{4}{3}\pi R^3 \frac{\mathrm{d}c}{\mathrm{d}t}\,\mathrm{d}R_0 = 0,$$

which leads, on using (12), to Eq. (8). Here we have assumed that $R_{0\max}$, $R_{0\min}$ are constants. Thus, for the continuous distribution of bubbles, in the quasistatic approximation, we again have the same system of Eqs. (9)–(11).

3. Boussinesq approximation

Let us introduce the dimensionless variables

$$\tilde{\rho} = \frac{\rho}{\rho_*}, \quad \tilde{p} = \frac{p}{\rho_* g h_*}, \quad \tilde{u} = \frac{u}{h_* N_*}, \quad \tilde{w} = \frac{w}{h_* N_*}, \quad \tilde{\alpha}_g = \frac{\alpha_g}{\sigma \alpha_*},$$
$$\tilde{t} = N_* t, \quad \tilde{x} = \frac{x}{h_*}, \quad \tilde{z} = \frac{z}{h_*},$$

where h_* is a typical depth of the stratified layer, N_* is a typical value of the buoyancy frequency in the mixture, ρ_* is a typical density value, and $\sigma\alpha_*$ is a typical value of the void fraction. Here, $\sigma = h_* N_*^2/g$ is the relevant Boussinesq parameter, which is very small in typical oceanic conditions, and so we will seek a reduced form of the model valid when $\sigma \ll 1$.

Then, Eqs. (9)–(11) assume the following non-dimensional form (the tilde superscripts are omitted):

$$\rho \frac{\mathrm{d}u}{\mathrm{d}t} + \frac{1}{\sigma} p_x = 0, \tag{14}$$

$$\rho \frac{\mathrm{d}w}{\mathrm{d}t} + \frac{1}{\sigma}(p_z + \rho) = 0, \tag{15}$$

$$\frac{1}{\rho}\frac{\mathrm{d}\rho}{\mathrm{d}t} = -\frac{\sigma\alpha_*}{1 - \sigma\alpha_*\alpha_g}\frac{\mathrm{d}\alpha_g}{\mathrm{d}t}, \tag{16}$$

$$u_x + w_z = \frac{\sigma\alpha_*}{1 - \sigma\alpha_*\alpha_g}\frac{\mathrm{d}\alpha_g}{\mathrm{d}t}, \tag{17}$$

$$\frac{\mathrm{d}}{\mathrm{d}t}\left(p^{1/\kappa}\alpha_g\right) + p^{1/\kappa}\alpha_g(u_x + w_z) = 0. \tag{18}$$

We will suppose that in the basic state the mixture has density $\rho_0(z)$, a corresponding pressure $p_0(z)$ (satisfying $p_{0z} = -\rho_0$), and that there is no shear flow, $u_0 = w_0 = 0$. The void fraction of bubbles in the basic state is also assumed to be a function of depth only: $\alpha_g = \alpha_{g0}(z)$. Here, we take into consideration only the vertical variability of the bubble layer and do not consider the horizontal spatial variations of its thickness, which in reality might be a significant feature. However, including such horizontal variability in the basic state leads to forbidding technical difficulties in analysing these equations, and so, as a first step, we focus here solely on the effects due to the vertical variability of the bubble layer.

We now perturb this basic state, assuming that

$$\rho = \rho_0(z) + \sigma\tilde{\rho}, \quad p = p_0(z) + \sigma\tilde{p}, \quad u = \tilde{u}, \quad w = \tilde{w},$$
$$\alpha_g = \alpha_{g0}(z) + \tilde{\alpha}_g.$$

Linearising Eqs. (14)–(18) about the basic state, we obtain, after omitting the tilde superscript,

$$\rho_0 u_t + p_x = 0, \tag{19}$$

$$\rho_0 w_t + p_z + \rho = 0, \tag{20}$$

$$\sigma\rho_t + \rho_{0z} w = -\frac{\rho_0 \sigma\alpha_*}{1-\sigma\alpha_*\alpha_{g0}}(\alpha_{gt} + \alpha_{g0z} w), \tag{21}$$

$$u_x + w_z = \frac{\sigma\alpha_*}{1-\sigma\alpha_*\alpha_{g0}}(\alpha_{gt} + \alpha_{g0z} w), \tag{22}$$

$$\sigma p_t + \frac{\kappa p_0}{\alpha_{g0}}\alpha_{gt} + \left(\kappa p_0 \frac{\alpha_{g0z}}{\alpha_{g0}} + p_{0z}\right) w + \kappa p_0 (u_x + w_z) = 0. \tag{23}$$

Note that here ρ_{0z} is $O(\sigma)$ so that all terms in (21) are of the same order.

This system can be reduced to just two equations for the variables w and α_g. The horizontal velocity u can be eliminated by taking the time derivative of (22) and using the horizontal momentum equation (19). This results in

$$\frac{1}{\rho_0} p_{xx} = w_{zt} - \frac{\sigma\alpha_*}{1-\sigma\alpha_*\alpha_{g0}}(\alpha_{gtt} + \alpha_{g0z} w_t). \tag{24}$$

We then take the time derivative of the vertical momentum equation (20) and use (21) to eliminate ρ, which leads to

$$\frac{1}{\rho_0} p_{zt} = -w_{tt} + \left(\frac{1}{\sigma}\frac{\rho_{0z}}{\rho_0} + \frac{\alpha_*\alpha_{g0z}}{1-\sigma\alpha_*\alpha_{g0}}\right) w + \frac{\alpha_*}{1-\sigma\alpha_*\alpha_{g0}}\alpha_{gt}. \tag{25}$$

Then, the pressure p can be eliminated by taking the second derivative of (25) with respect to x and second derivative of (24) with respect to z and t. In the usual Boussinesq approximation (neglecting $(1/\rho_0)_z p_{xxt}$ term) this gives

$$\frac{\partial^2}{\partial t^2}(w_{xx} + w_{zz}) - \left(\frac{1}{\sigma}\frac{\rho_{0z}}{\rho_0} + \frac{\alpha_*\alpha_{g0z}}{1-\sigma\alpha_*\alpha_{g0}}\right) w_{xx} - \frac{\alpha_*}{1-\sigma\alpha_*\alpha_{g0}}\alpha_{gtxx} - \left[\frac{\sigma\alpha_*}{1-\sigma\alpha_*\alpha_{g0}}(\alpha_{gttt} + \alpha_{g0z} w_{tt})\right]_z = 0. \tag{26}$$

To derive the second equation, we first use (22) and rewrite (23) as

$$\sigma p_t + \frac{\kappa p_0}{\alpha_{g0}(1-\sigma\alpha_*\alpha_{g0})}\alpha_{gt} + \left(\frac{\kappa p_0 \alpha_{g0z}}{\alpha_{g0}(1-\sigma\alpha_*\alpha_{g0})} + p_{0z}\right) w = 0. \tag{27}$$

Then, by taking the second derivative of (27) with respect to x and using (24) to exclude p, we obtain the second equation:

$$\left(\frac{\kappa p_0 \alpha_{g0z}}{\alpha_{g0}(1-\sigma\alpha_*\alpha_{g0})} + p_{0z}\right) w_{xx} + \frac{\kappa p_0}{\alpha_{g0}(1-\sigma\alpha_*\alpha_{g0})}\alpha_{gtxx} + \sigma\rho_0\left[w_{ztt} - \frac{\sigma\alpha_*}{1-\sigma\alpha_*\alpha_{g0}}(\alpha_{gttt} + \alpha_{g0z} w_{tt})\right] = 0. \tag{28}$$

We now use the Boussinesq approximation, so that $\sigma \ll 1$. In this case (26) becomes

$$\frac{\partial^2}{\partial t^2}(w_{xx} + w_{zz}) - \left(\frac{1}{\sigma}\frac{\rho_{0z}}{\rho_0} + \alpha_*\alpha_{g0z}\right) w_{xx} - \alpha_*\alpha_{gtxx} = 0. \tag{29}$$

Next from (28) we obtain, likewise in the Boussinesq approximation,

$$\frac{\kappa p_0}{\alpha_{g0}}\alpha_{gtxx} + \left(\kappa p_0 \frac{\alpha_{g0z}}{\alpha_{g0}} + p_{0z}\right) w_{xx} = 0. \tag{30}$$

Substituting (30) into (29), we finally get a single equation for the internal wave mode,

$$\frac{\partial^2}{\partial t^2}(w_{xx} + w_{zz}) + N^2_{\text{eff}}(z) w_{xx} = 0, \tag{31}$$

where the value of the buoyancy frequency in the fluid should be replaced by the effective buoyancy frequency

$$N_{\rm eff}^2(z) = -\frac{1}{\sigma}\frac{\rho_{0z}}{\rho_0} + \frac{\alpha_*\alpha_{g0}}{\kappa}\frac{p_{0z}}{p_0}. \tag{32}$$

Note that Eq. (31) can be obtained by dropping the $\mathrm{O}(\sigma)$ terms in all Eqs (19)–(23) except (21) from the outset, similar to the use of the Boussinesq approximation in the absence of any bubbles.

Taking into account that $\rho_0 = \rho_{l0}(1-\sigma\alpha_*\alpha_{g0})$ and $p_{0z} = -\rho_0$, (32) yields

$$N_{\rm eff}^2(z) = -\frac{1}{\sigma}\frac{\rho_{l0z}}{\rho_{l0}} + \alpha_*\alpha_{g0z} - \frac{\alpha_*\alpha_{g0}}{\kappa}\frac{\rho_{l0}}{p_{l0}} + \mathrm{O}(\sigma),$$

where $p_{l0z} = -\rho_{l0}$. Returning to the dimensional variables, we obtain, in the Boussinesq approximation,

$$N_{\rm eff}^2(z) = -g\frac{\rho_{l0z}}{\rho_{l0}} + g\alpha_{g0z} - \frac{g^2\rho_{l0}\alpha_{g0}}{\kappa p_{l0}} = N_l^2 + g\alpha_{g0z} - \frac{g^2\rho_{l0}\alpha_{g0}}{\kappa p_{l0}}, \tag{33}$$

where $p_{l0z} = -g\rho_{l0}$. Here $N_l^2 = -g\rho_{l0z}/\rho_{l0}$ is the value of the buoyancy frequency in the pure fluid.

The formula (33) reflects two physical factors affecting the buoyancy frequency in the mixture; the effective stratification due to the bubbles, expressed in the second term in (33), adds to the stratification in the pure fluid, while the compressibility of the mixture due to the bubbles, expressed in the third term in (33) reduces the pure buoyancy frequency. Considering possible applications to oceanic conditions, let the buoyancy frequency of the pure fluid lie in the range $N_l \approx 10^{-3}$–10^{-2} s^{-1} (e.g., Gill [4]). Let us assume an exponential decay of the void fraction, so that $\alpha_{g0z} = \gamma\alpha_{g0}$ where $\gamma \approx 0.5$–1.0 m^{-1} (e.g., Buckingham [12]). Also, suppose that over this thin bubble layer, $\rho_0 \approx 10^3$ kg m^{-3}, $p_0 \approx 10^5$ Pa are both approximately constant, and $\kappa = 1.4$, $g = 9.8$ m s^{-2}.Then, we estimate the second term in (33) to be $\mathrm{O}((5-10)\alpha_{g0})$, depending on the value of γ, that is, on the e-folding scale of the bubble layer, while the third term is $\mathrm{O}(\alpha_{g0})$. Thus, there may be an anomalously high value of the effective buoyancy frequency in the upper mixed layer due to the depth-dependent distribution of bubbles, compared to the situation without the bubbles. Typically if the void fraction α_{g0} is in the range 10^{-5} to 10^{-3}, then the corrections to N_l are comparable with N_l itself (see the estimates above). Further, for these typical oceanic conditions, the correction to the buoyancy frequency due to the bubble stratification is considerably larger than the correction due to the compressibility of the bubble mixture. But, also let us note that this comparison may fail for smaller values of γ; we estimate that the two terms become comparable for $\gamma \approx 0.1$ m^{-1} when the bubble layer has an e-folding scale of order 10 m. However, for the distributions observed in the ocean $\gamma \approx 0.5$–1.0 m^{-1} (see above). We shall return to this issue in the next section.

4. Normal modes

In the present Boussinesq approximation equation (31) is supplemented by the usual surface and bottom boundary conditions for internal waves:

$$w|_{z=0} = 0, \qquad w|_{z=-H} = 0.$$

That is, as well as a rigid flat bottom, the free surface is approximated by a rigid lid in the usual way.

We look for solutions of (31) in the form

$$w = \phi(z)\exp\bigl[\mathrm{i}(kx-\omega t)\bigr] + c.c.,$$

which leads to the Sturm–Liouville problem

$$\frac{\mathrm{d}^2\phi}{\mathrm{d}z^2} + \frac{k^2(N_{\rm eff}^2(z)-\omega^2)}{\omega^2}\phi = 0,$$

where

$$\phi|_{z=0} = 0, \qquad \phi|_{z=-H} = 0.$$

Here, we recall that $N_{\rm eff}^2(z)$ is defined by (33). It is well known (e.g., Miropol'sky [5]) that this boundary value problem typically has countably many solutions (modes), characterised by their dispersion curves:

$$\omega = \omega_n(k), \quad n = 1, 2, 3, \ldots.$$

Each such curve is a monotonic function of k, $0 < \omega_n(k) < \mu$, and $\lim_{k\to\infty} \omega_n = \mu$, where μ is the maximum of $N_{\rm eff}(z)$ on the interval $[-H, 0]$.

Since the bubble layer is essentially near the surface, and usually has a vertical length scale much less than that of the underlying basic density stratification, a multiscale analysis of this problem could presumably be developed. However, in the following subsections we choose to look instead at three different cases, where explicit expressions can be obtained, to demonstrate the effect of the bubble layer on the internal wave dynamics over a full range of possible length scales.

4.1. Uniform density stratification

Here we examine the case when the pure fluid has a constant buoyancy frequency, that is $N_l = const$, which is perhaps one of the simplest models used to represent the oceanic density stratification. An important special case arises here when in fact $N_l = 0$ so that the density stratification is entirely due to the bubbles. In this situation we will show that bubble distributions observed in the ocean can themselves support internal wave modes, which we will call *bubble* modes. We then restore the background fluid stratification, that is $N_l = const \neq 0$, so that the oceanic waveguide can support internal wave modes in the absence of any bubbles. In this situation, we then explore how the two waveguides can interact with each other.

Since the buoyancy frequency N_l is a constant (possibly zero) the density of the fluid is given by

$$\rho_{l0} = \rho_a \mathrm{e}^{-(N_l^2/g)z},$$

where ρ_a is the density at the free surface. For oceanic conditions, the void fraction either decays exponentially, or follows the inverse square law (see the Introduction). Here, we assume an exponential dependence $\alpha_{g0} = \alpha_a \mathrm{e}^{\gamma z}$, with $\gamma \approx 0.5$–$1.0\ \mathrm{m}^{-1}$ (Buckingham [12]) and α_a is the value of the void fraction close to the free surface. The pressure p_{l0} is given by

$$p_{l0} = p_a + \frac{\rho_a g^2}{N_l^2}\left(\mathrm{e}^{-(N_l^2/g)z} - 1\right),$$

where p_a is the atmospheric pressure.

This leads to the following expression for the effective buoyancy frequency:

$$N_{\rm eff}^2(z) = N_l^2 + N_g^2(z) - N_c^2(z), \tag{34}$$

$$\text{where } N_g^2(z) = g\gamma\alpha_a \mathrm{e}^{\gamma z}, \quad N_c^2(z) = \varepsilon g\gamma\alpha_a \tilde{P}(z),$$

$$\tilde{P}(z) = \frac{p_a \mathrm{e}^{(\gamma - \frac{N_l^2}{g})z}}{p_{l0}}, \qquad \varepsilon = \frac{\rho_a g}{\gamma\kappa p_a}. \tag{35}$$

Here, $N_g^2(z)$ denotes the contribution due to the effective stratification in the presence of bubbles, and $N_c^2(z)$ denotes the contribution due to the compressibility of the mixture. For the typical oceanic conditions, $\rho_a = 10^3\ \mathrm{kg\,m^{-3}}$, $g = 9.8\ \mathrm{m\,s^{-2}}$, $\gamma = 0.5$–$1.0\ \mathrm{m}^{-1}$, $\kappa = 1.4$, $p_a = 10^5\ \mathrm{N\,m^{-2}}$, which leads to $\varepsilon \approx 0.07$–0.14. Thus, the modal equation (4) takes the form

$$\frac{\mathrm{d}^2\phi}{\mathrm{d}z^2} + \frac{k^2(N_l^2 + g\gamma\alpha_a \mathrm{e}^{\gamma z} - \omega^2)}{\omega^2}\phi = \varepsilon \frac{k^2}{\omega^2} g\gamma\alpha_a \tilde{P}(z)\phi, \tag{36}$$

where the term on the right-hand side can be treated as a perturbation of the main terms on the left-hand side.

We look for solutions of (36) in the form

$$\phi = \phi_0 + \varepsilon\tilde{\phi} + \mathrm{O}\left(\varepsilon^2\right), \qquad \omega^2 = \omega_0^2 + \varepsilon\lambda + \mathrm{O}\left(\varepsilon^2\right), \tag{37}$$

which to the leading order yields

$$\frac{\mathrm{d}^2\phi_0}{\mathrm{d}z^2} + \frac{k^2(N_l^2 + g\gamma\alpha_a \mathrm{e}^{\gamma z} - \omega_0^2)}{\omega_0^2}\phi_0 = 0, \tag{38}$$

$$\phi_0|_{z=0} = 0, \qquad \phi_0|_{z=-H} = 0.$$

Let us make a change of variable:

$$\tilde{z} = 2\sqrt{a}\,\mathrm{e}^{\gamma z/2}, \quad a = g\alpha_a k^2/(\gamma\omega_0^2),$$

which reduces the unperturbed equation (38) to the Bessel equation (e.g., Abramowitz and Stegun [21])

$$\tilde{z}^2\phi_0'' + \tilde{z}\phi_0' + \bigl(\tilde{z}^2 - \nu^2\bigr)\phi_0 = 0, \quad \nu^2 = \frac{4k^2(\omega_0^2 - N_l^2)}{\gamma^2\omega_0^2}. \tag{39}$$

This equation is supplemented by the boundary conditions

$$\phi_0|_{\tilde{z}=2\sqrt{a}} = 0, \qquad \phi_0|_{\tilde{z}=2\sqrt{a}\,\mathrm{e}^{-\gamma H/2}} = 0. \tag{40}$$

The general solution of (39) is given by

$$\phi_0(\tilde{z}) = C_1 J_\nu(\tilde{z}) + C_2 Y_\nu(\tilde{z}), \tag{41}$$

where J_ν and Y_ν are Bessel functions of the first and second kind. Note, that for $\omega_0 < N_l$ the order ν of the Bessel functions will be purely imaginary. For $N_l < \omega_0 < \mu$, the parameter ν and the Bessel functions of the corresponding order are real-valued.

The boundary conditions (55) imply that the dispersion curves $\omega_0 = \omega_{0n}(k)$, $n = 1, 2, 3, \ldots$, for the internal modes are given by the roots of the expression,

$$J_\nu(2\sqrt{a})Y_\nu\bigl(2\sqrt{a}\,\mathrm{e}^{-\gamma H/2}\bigr) - Y_\nu\bigl(2\sqrt{a}\bigr)J_\nu\bigl(2\sqrt{a}\,\mathrm{e}^{-\gamma H/2}\bigr) = 0. \tag{42}$$

The non-normalised real-valued modal functions of the problem (38) can be written in the form

$$\phi_{0n}(z) = Y_{\nu_n}(2\sqrt{a_n})J_{\nu_n}\bigl(2\sqrt{a_n}\,\mathrm{e}^{\gamma z/2}\bigr) - J_{\nu_n}\bigl(2\sqrt{a_n}\bigr)Y_{\nu_n}\bigl(2\sqrt{a_n}\,\mathrm{e}^{\gamma z/2}\bigr) + c.c. \quad (n = 1, 2, 3, \ldots). \tag{43}$$

Before proceeding, let us mention that in the limit to the pure fluid situation, i.e. $\alpha_a \to 0$, the dispersion relation (42) reduces to the usual dispersion relation for internal wave modes (in the following we write ω instead of ω_0)

$$\omega^2 = \frac{k^2 N_l^2}{k^2 + (n\pi/H)^2}, \tag{44}$$

with $n = 1, 2, 3 \ldots$. Indeed, for a small fixed value of α_a and fixed values of k and ω, the parameter $a = g\alpha_a k^2/(\gamma\omega^2)$ is also small. Then, using the standard expansions of the Bessel functions in the vicinity of zero (e.g., Abramowitz and Stegun [21]) and considering the limit $\alpha_a \to 0$, we obtain

$$\sinh\frac{\gamma\nu H}{2} = 0. \tag{45}$$

Here, $\gamma\nu/2 = k\sqrt{\omega^2 - N_l^2}/\omega$. For the real non-zero values of this parameter, Eq. (45) has no solutions. Therefore, one has to consider the imaginary values,

$$\frac{k}{\omega}\sqrt{\omega^2 - N_l^2} = \mathrm{i}l, \tag{46}$$

which leads to the equation $\sin lH = 0$ instead of (45). This equation has countably many solutions $lH = n\pi$, for the integer values of n. Then, substituting these values into Eq. (46), one obtains (44).

Let us now consider the opposite case when the stratification is entirely due to the bubbles, that is, we assume that $N_l = 0$, i.e. $\rho_{l0} = \rho_a = \text{constant}$. This leads to the following expression for the effective buoyancy frequency

$$N_{\text{eff}}^2(z) = g\gamma\alpha_a \mathrm{e}^{\gamma z}\bigl[1 - \varepsilon\tilde{Q}(z)\bigr], \tag{47}$$

where

$$\tilde{Q}(z) = \frac{p_a}{p_a - \rho_a g z}.$$

Here, we again consider just the leading order problem, when $\varepsilon \to 0$. The effect of the compressibility term will be estimated later.

In this case, the order ν of the Bessel functions in (43) is real. The roots of the dispersion equation (42) are real and simple (e.g., Tranter [22]). An asymptotic formula can be written down for the high order zeros of this equation (e.g.,

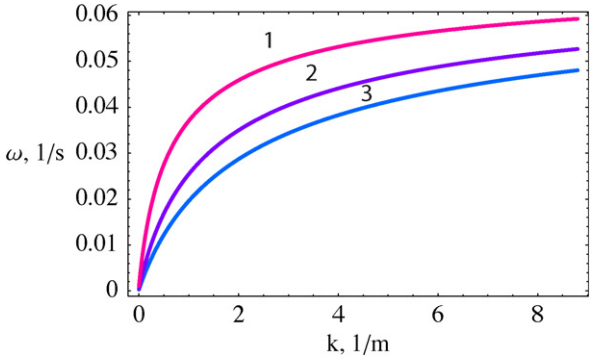

Fig. 1. The first three dispersion curves for $H = 100$ m, $\gamma = 0.5$ m^{-1}, $\alpha_a = 0.001$.

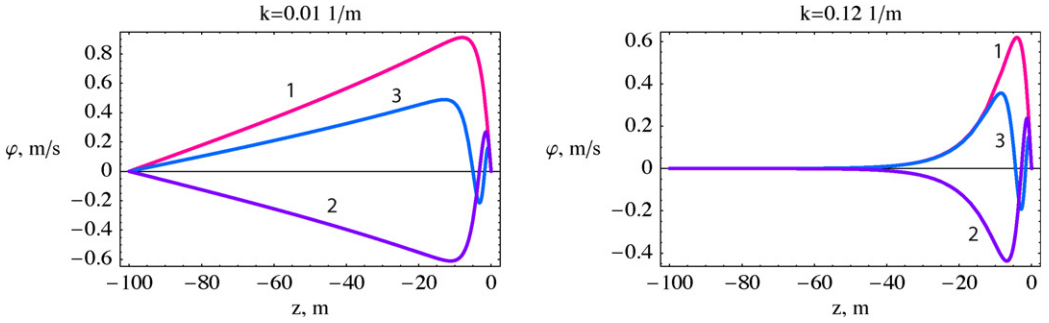

Fig. 2. The first three modal functions for $H = 100$ m, $\gamma = 0.5$ m^{-1}, $\alpha_a = 0.001$.

Abramowitz and Stegun [23]). However, only the first modes are interesting from a physical point of view. Above we show the dispersion curves (42) for the first three modes, obtained numerically, for a realistic set of parameters: $H = 100$ m, $\gamma = 0.5$ m^{-1}, $\alpha_a = 0.001$ (Fig. 1).

Here the modes are indexed in the usual way, by the increasing number of internal zeros of the modal functions. These are plotted in Fig. 2 for the corresponding dispersion curves shown in Fig. 1, for two different values of the wavenumber k: $k = 0.01$ m^{-1} and $k = 0.12$ m^{-1}. Thus, a depth-dependent distribution of bubbles leads to the existence of internal modes in an otherwise homogeneous fluid. It is interesting to note that although the void fraction of bubbles decays rather rapidly with depth, the modes shown in Fig. 2 are not trapped in the very upper part of the waveguide. Instead, they are still present at a considerable depth. For the cases shown, this is because the waves are long compared to the depth of the bubble layer ($k/\gamma = 0.02, 0.24$ respectively), although they are not long waves compared to the total depth ($kH = 1, 12$ respectively). Only very short internal waves, with $k \geqslant \gamma^{-1}$, will have modes trapped within the bubble layer. We also examined the case when $H = 500$ m, with all the other parameters unchanged. The dispersion curves are qualitatively unchanged, with some small quantitative differences arising only for very small values of k. Since now $kH = 5, 60$ respectively, the modes do not "feel" the bottom, and instead decay in the deeper water as k^{-1}. For the case of $k = 0.12$ m^{-1} there is a no observable change in the modal structure; for the case $k = 0.01$ m^{-1} while there is no observable qualitative change in the modal structure in the bubble layer, there is a minor qualitative difference in the modal structure in the deeper water, where now the decay is exponential rather than the near-linear decay shown in Fig. 2.

Let us next assume that there is a uniform background fluid stratification $N_l = const$. In this case, we have two weakly interacting waveguides; the main internal waveguide due to the stratification of the fluid, and the additional bubble waveguide due to the depth-dependent distribution of bubbles in the upper part of the fluid. As we have demonstrated above, each of them separately can support wave modes that have their own dispersion curves. In the absence of any coupling, the corresponding dispersion curves would intersect at some finite k. The weak coupling present induces a splitting of the dispersion curves, clearly seen in Fig. 3 for $N_l = 0.015$ s^{-1} and the same values of other parameters as in Fig. 1 (that is, $H = 100$ m, $\gamma = 0.5$ m^{-1}, $\alpha_a = 0.001$). Thus, for instance, the first dispersion curve follows the dispersion curve of the main internal waveguide, but soon after the inflection point where there is

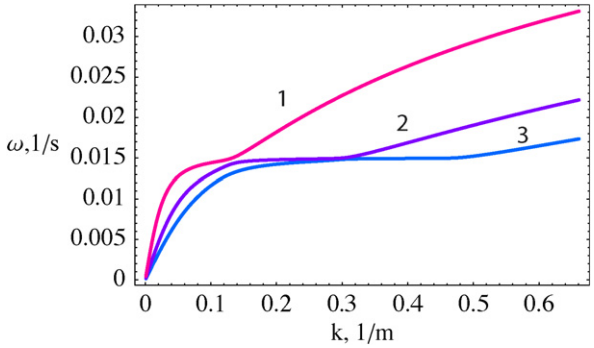

Fig. 3. The first three dispersion curves for $H = 100$ m, $\gamma = 0.5$ m^{-1}, $\alpha_a = 0.001$, $N_l = 0.015$ s^{-1}.

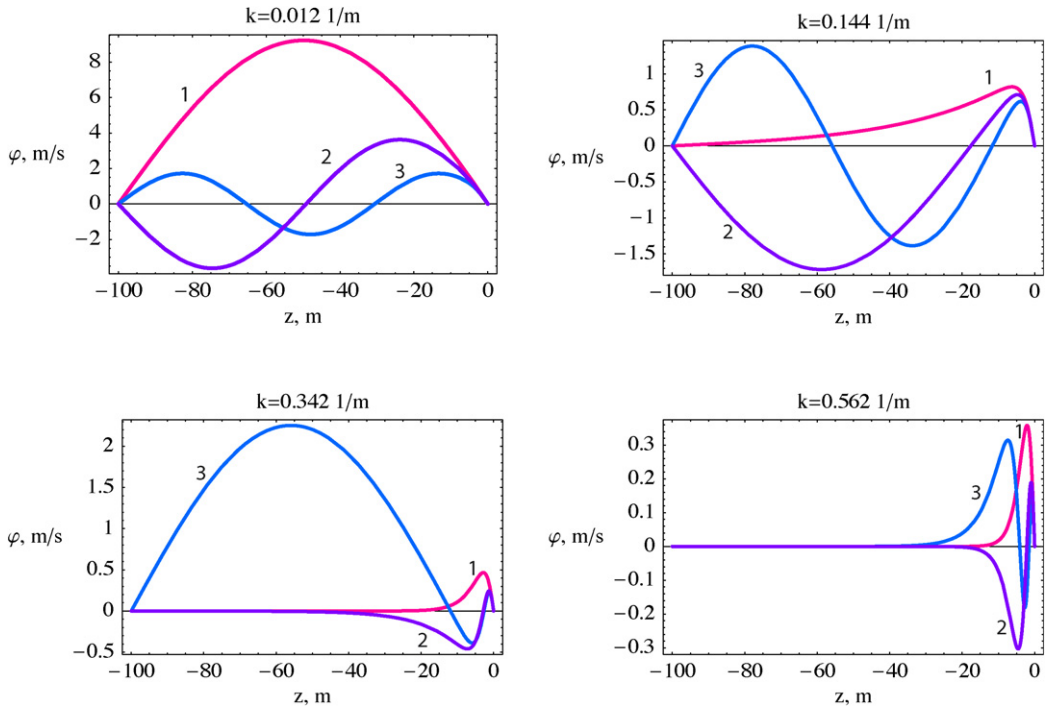

Fig. 4. The first three modal functions for $H = 100$ m, $\gamma = 0.5$ m^{-1}, $\alpha_a = 0.001$, $N_l = 0.015$ s^{-1}.

a close encounter with the second dispersion curve, it continues as the dispersion curve of the bubble waveguide. An analogous situation holds for the second and third dispersion curves. Such situation is typical for weakly interacting waveguides, and is often referred to as a near-"kissing" event.

The behaviour of the dispersion curves is reflected in the behaviour of the corresponding modal functions, shown in Fig. 4 for four different values of the wavenumber k: $k = 0.012$ m^{-1}, $k = 0.144$ m^{-1}, $k = 0.342$ m^{-1} and $k = 0.562$ m^{-1}. Before the inflection points of the dispersion curves (e.g., $k = 0.012$ m^{-1}), the modes occupy the entire fluid waveguide, but the behaviour after the inflection points is different. For example, in the vicinity of the inflection point of the first mode ($k = 0.144$ m^{-1}), the first mode becomes trapped in the bubble waveguide, while the second and the third still occupy the entire depth. The same transition occurs for the second and the third modes near the inflection points of the respective dispersion curves ($k = 0.342$ m^{-1} and $k = 0.562$ m^{-1}). For the last value, $k = 0.562$ m^{-1}, all three modes are trapped in the bubble waveguide. Again, we also examined the case when $H = 500$ m, with all the other parameters unchanged, and the dispersion curves are shown in Fig. 5. They are qualitatively the same as that shown in Fig. 3, but because the difference between the "internal" mode occupying the whole depth and the "bubble" mode confined to the bubble layer is now more greatly accentuated, the near-"kissing" struc-

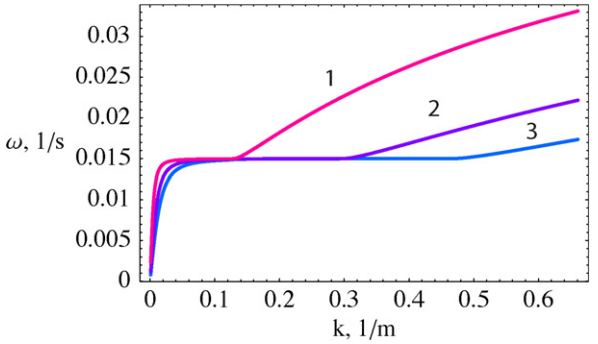

Fig. 5. The first three dispersion curves for $H = 500$ m, $\gamma = 0.5\ \mathrm{m}^{-1}$, $\alpha_a = 0.001$, $N_l = 0.015\ \mathrm{s}^{-1}$.

ture at the inflection points is consequently more prominent. The modal functions have much the same structure in the bubble layer, but in the deeper water now differ from those shown in Fig. 4; indeed, since the oscillatory structure in the deeper water extends over the whole depth, the modes have essentially the same shape as those shown in Fig. 4, but are rescaled to fit the whole domain. We also examined cases with weaker background fluid stratification (e.g., $N_l = 0.01\ \mathrm{s}^{-1}$), with no qualitative change in the behaviour of both the dispersion curves and the modal functions.

We next use a perturbation theory to estimate the effect of compressibility on the dispersion relation. To find the first corrections to ω_0^2 and ϕ_0 (see expansions (37)), one has to solve the following inhomogeneous problem:

$$\frac{\mathrm{d}^2\tilde{\phi}}{\mathrm{d}z^2} + \frac{k^2(N_l^2 + g\gamma\alpha_a \mathrm{e}^{\gamma z} - \omega_0^2)}{\omega_0^2}\tilde{\phi} = \frac{k^2}{\omega_0^2}\left(g\gamma\alpha_a \tilde{P}(z) + \lambda\frac{N_l^2 + g\gamma\alpha_a \mathrm{e}^{\gamma z}}{\omega_0^2}\right)\phi_0, \tag{48}$$

$$\tilde{\phi}|_{z=0} = 0, \qquad \tilde{\phi}|_{z=-H} = 0.$$

The solvability condition for this problem requires the orthogonality of the right-hand side of (48) to the solution ϕ_0 of the homogeneous problem, which leads to the following expression for the first correction to the dispersion relation for the modes,

$$\frac{\lambda(k,\omega_0)}{\omega_0^2} = -\frac{g\gamma\alpha_a \int_{-H}^{0} \tilde{P}(z)\phi_0^2(z)\,\mathrm{d}z}{\int_{-H}^{0}(N_l^2 + g\gamma\alpha_a\,\mathrm{e}^{\gamma z})\phi_0^2(z)\,\mathrm{d}z}, \quad \omega_0 = \omega_{n0}(k),\ n = 1, 2, 3, \ldots. \tag{49}$$

From (35), it is readily shown that, since $N_l \geqslant 0$ and $z \leqslant 0$,

$$g\gamma\alpha_a \tilde{P}(z) = \frac{g\gamma\alpha_a p_a \mathrm{e}^{(\gamma - N_l^2/g)z}}{p_a + (\rho_a g^2/N_l^2)(\mathrm{e}^{-(N_l^2/g)z} - 1)} \leqslant \frac{g\gamma\alpha_a p_a \mathrm{e}^{(\gamma - N_l^2/g)z} + p_a N_l^2}{p_a} \leqslant N_l^2 + g\gamma\alpha_a \mathrm{e}^{\gamma z}.$$

Then, taking into account that both integrands in (49) are non-negative in the interval $[-H, 0]$, we deduce that

$$\left|\frac{\lambda(k,\omega_0)}{\omega_0^2}\right| \leqslant 1.$$

Thus, for a fixed k, compressibility results in decreasing the frequency compared to ω_0, but the value of the correction to ω_0^2 due to this effect is $\varepsilon\lambda(k,\omega_0)$ (see (37)), and, thus, is small (in typical oceanic conditions, $\varepsilon \approx 0.07$–0.14, see above). Hence, it seems that in the oceanic context compressibility effects can usually be ignored.

4.2. Two-layer model

The considerations of the previous subsection can be viewed as a generalisation of the classical problem of internal wave modes in a fluid with constant buoyancy frequency. In this section we address the question, how does the bubble layer effect internal wave modes, when there is a sharp pycnocline below the free surface. As a first step in this direction we consider the simplest and commonly-used model, a two-layer fluid, where we have just one pycnocline mode in the absence of any bubbles. The upper layer has an undisturbed constant depth h, a constant density ρ_1 in the absence of any bubbles, and a near surface bubble distribution, while the lower layer is without bubbles and has

a constant density ρ_2. For simplicity, we assume this layer to have infinite depth. Previously, we have considered a two- and three-layer models, where all layers had constant but different effective buoyancy frequencies (Grimshaw and Khusnutdinova [1,2]). Here, we do not require the effective buoyancy frequency in the upper layer to be constant, considering as before the case of an exponentially decaying distributions of bubbles.

The relevant equations and boundary conditions follow, where subscript 1(2) corresponds to the upper (lower) layer. The boundary conditions on the top and at the bottom then are

$$w_1|_{z=0} = 0, \quad w_2 \to 0 \quad \text{at } z \to -\infty. \tag{50}$$

The linearised conditions at the interface are

$$w_1|_{z=-h} = w_2|_{z=-h} = \zeta_t \quad \text{and} \tag{51}$$

$$p_1 - p_2|_{z=-h} = -(\rho_2 - \rho_1) g\zeta, \tag{52}$$

where $\zeta(x,t)$ is the interface displacement, respectively expressing continuity of the vertical displacement and the pressure. In the Boussinesq approximation used to derive Eq. (31) condition (52) takes the form

$$w_{1zt} - w_{2zt}|_{z=-h} = -\Delta\rho g \zeta_{xx}, \quad \text{where } \Delta\rho = \frac{\rho_2 - \rho_1}{\rho_1}. \tag{53}$$

Note that we have assumed here that $\rho_2 - \rho_1$ is $O(\sigma)$. In the lower layer (pure homogeneous fluid without bubbles) we have just Laplace's equation for w_2. The solution which satisfies (57) is

$$w_2 = C \exp\bigl[k(z+h)\bigr] \exp\bigl[\mathrm{i}(kx - \omega t)\bigr] + c.c.$$

Assuming that $\zeta(x,t) = A \exp[\mathrm{i}(kx - \omega t)] + c.c.$ and applying the boundary condition at the interface, we get

$$C = -\mathrm{i}\omega A.$$

In the upper layer we have (31) as in Section 3, where N_{eff} is given by (34) and takes the form (in the appropriate limit)

$$N^2_{\mathrm{eff}}(z) = N^2_g(z) - N^2_c(z), \quad \text{where } N^2_g(z) = g\gamma\alpha_a \mathrm{e}^{\gamma z},\ N^2_c(z) = \varepsilon g\gamma\alpha_a \tilde{P}(z),$$

$$\tilde{P} = \frac{p_a \mathrm{e}^{\gamma z}}{p_a - \rho_1 g z}, \qquad \varepsilon = \frac{\rho_1 g}{\gamma \kappa p_a}.$$

As before, $N^2_g(z)$ denotes the contribution due to the effective stratification in the presence of bubbles, and $N^2_c(z)$ denotes the contribution due to the compressibility of the mixture.

Again we look for a solution of (4) in the form (37) and at the leading order the Sturm–Liouville problem (36) now reduces to

$$\frac{\mathrm{d}^2\phi_0}{\mathrm{d}z^2} + \frac{k^2(g\gamma\alpha_a \mathrm{e}^{\gamma z} - \omega_0^2)}{\omega_0^2}\phi_0 = 0,$$

$$\phi_0|_{z=0} = 0, \qquad \phi_0|_{z=-h} = -\mathrm{i}\omega A.$$

Making the same change of variable as before,

$$\tilde{z} = 2\sqrt{a}\, \mathrm{e}^{\gamma z/2},$$

where $a = g\alpha_a k^2/(\gamma\omega_0^2)$, we obtain

$$\tilde{z}^2\phi_0'' + \tilde{z}\phi_0' + \bigl(\tilde{z}^2 - \nu^2\bigr)\phi_0 = 0, \quad \nu = \frac{2k}{\gamma}. \tag{54}$$

This equation is supplemented by the boundary conditions

$$\phi_0|_{\tilde{z}=2\sqrt{a}} = 0, \qquad \phi_0|_{\tilde{z}=2\sqrt{a}\,\mathrm{e}^{-\gamma h/2}} = -\mathrm{i}\omega A. \tag{55}$$

The general solution of (54) is again given by

$$\phi_0(\tilde{z}) = C_1 J_\nu(\tilde{z}) + C_2 Y_\nu(\tilde{z}),$$

while the boundary conditions now imply that

$$C_1 = \frac{-\mathrm{i}\omega A Y_\nu(2\sqrt{a})}{Y_\nu(2\sqrt{a})J_\nu(2\sqrt{a}\,\mathrm{e}^{-\gamma h/2}) - J_\nu(2\sqrt{a})Y_\nu(2\sqrt{a}\,\mathrm{e}^{-\gamma h/2})},$$

$$C_2 = \frac{\mathrm{i}\omega A J_\nu(2\sqrt{a})}{Y_\nu(2\sqrt{a})J_\nu(2\sqrt{a}\,\mathrm{e}^{-\gamma h/2}) - J_\nu(2\sqrt{a})Y_\nu(2\sqrt{a}\,\mathrm{e}^{-\gamma h/2})}.$$

Finally the pressure condition (53) implies that the dispersion curves $\omega_0 = \omega_{0n}(k)$ $(n = 1, 2, 3, \ldots)$ for the internal modes are given by the roots of the following equation:

$$\omega^2\left[k - \gamma\sqrt{a}\exp\left(-\frac{\gamma h}{2}\right)\frac{Y_\nu(2\sqrt{a})J'_\nu(2\sqrt{a}\,\mathrm{e}^{-\gamma h/2}) - J_\nu(2\sqrt{a})Y'_\nu(2\sqrt{a}\,\mathrm{e}^{-\gamma h/2})}{Y_\nu(2\sqrt{a})J_\nu(2\sqrt{a}\,\mathrm{e}^{-\gamma h/2}) - J_\nu(2\sqrt{a})Y_\nu(2\sqrt{a}\,\mathrm{e}^{-\gamma h/2})}\right] = g\Delta\rho k^2, \tag{56}$$

where the prime denotes differentiation with respect to the argument of the function. In the limit to the pure fluid situation ($\alpha_a \to 0$) this dispersion relation reduces to (in the following we write ω instead of ω_0)

$$\omega^2 = \frac{g\Delta\rho k}{1 + \coth kh},$$

which for $kh \ll 1$ gives $\omega^2 = g\Delta\rho hk^2$, and for $kh \gg 1$ it gives $\omega^2 = g\Delta\rho k/2$.

Since here the parameter ν and the corresponding Bessel functions are real-valued, the corresponding modal functions in the upper layer assume the following (non-normalised) form

$$\phi_{0n}(z) = Y_{\nu_n}\left(2\sqrt{a_n}\right)J_{\nu_n}\left(2\sqrt{a_n}\,\mathrm{e}^{\gamma z/2}\right) - J_{\nu_n}\left(2\sqrt{a_n}\right)Y_{\nu_n}\left(2\sqrt{a_n}\,\mathrm{e}^{\gamma z/2}\right) \quad (n = 1, 2, 3, \ldots).$$

This dispersion relation (56) is solved numerically, and in Figs. 6 and 7 we show the dispersion curves for the first four modes, for a shallow pycnocline, where $h = 5$ m, $\gamma = 1\ \mathrm{m}^{-1}$, $\Delta\rho = 0.001$ and $\alpha_a = 0.01$ (Fig. 6) and $\alpha_a = 0.005$ (Fig. 7). In both figures the pure pycnocline mode (in the absence of any bubbles) is shown by a dashed line.

The splitting of the dispersion curves is again seen in both figures but is more prominent in Fig. 6, which corresponds to the case of a shallow pycnocline and a relatively large void fraction of bubbles. For a weaker interaction between bubble modes and a pycnocline mode, which corresponds to a deeper pycnocline, larger density jump or smaller void fractions of bubbles (as in Fig. 7), the splitting of the dispersion curves is still present, but less pronounced, resulting in a pycnocline mode now looking much as the same as the bubble modes. Finally, if the pycnocline is well separated from the bubble layer, then there is virtually no interaction of the pycnocline mode with the bubble modes, and we have two independent waveguides at different depths. This happens in cases of a deeper pycnocline, small void fractions of bubbles or a strong density jump (as in Fig. 8, where $\Delta\rho = 0.01$ and all other parameters are the same as in Fig. 7).

The modal functions in the upper layer corresponding to the dispersion curves shown in Fig. 6 are plotted in Fig. 9 for three different values of the wavenumber k: $k = 0.012\ \mathrm{m}^{-1}$, $k = 0.441\ \mathrm{m}^{-1}$ and $k = 1.100\ \mathrm{m}^{-1}$. In these plots, the pycnocline mode should be identified with the first, second and third dispersion curves, respectively, in accordance with the behaviour of the dispersion curves.

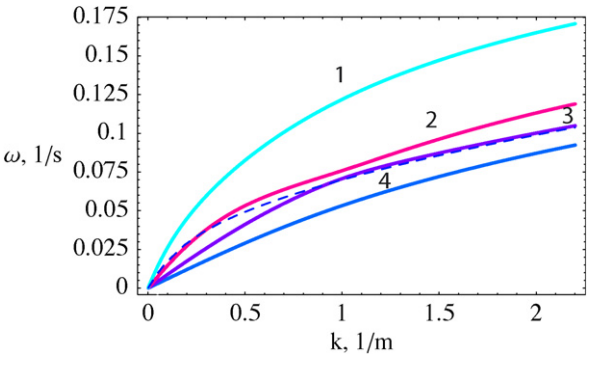

Fig. 6. The first four dispersion curves for $h = 5$ m, $\gamma = 1\ \mathrm{m}^{-1}$, $\alpha_a = 0.01$, $\Delta\rho = 0.001$.

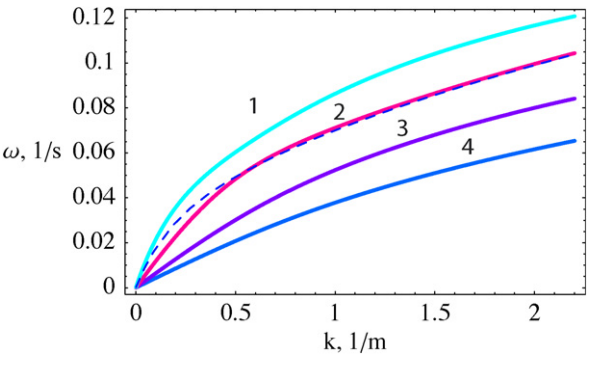

Fig. 7. The first four dispersion curves for $h = 5$ m, $\gamma = 1\ \mathrm{m}^{-1}$, $\alpha_a = 0.005$, $\Delta\rho = 0.001$.

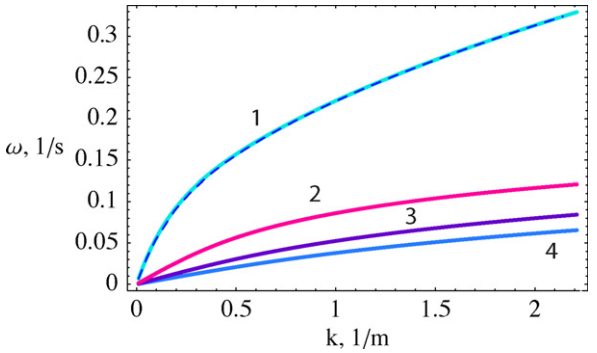

Fig. 8. The first four dispersion curves for $h = 5$ m, $\gamma = 1$ m^{-1}, $\alpha_a = 0.005$, $\Delta\rho = 0.01$.

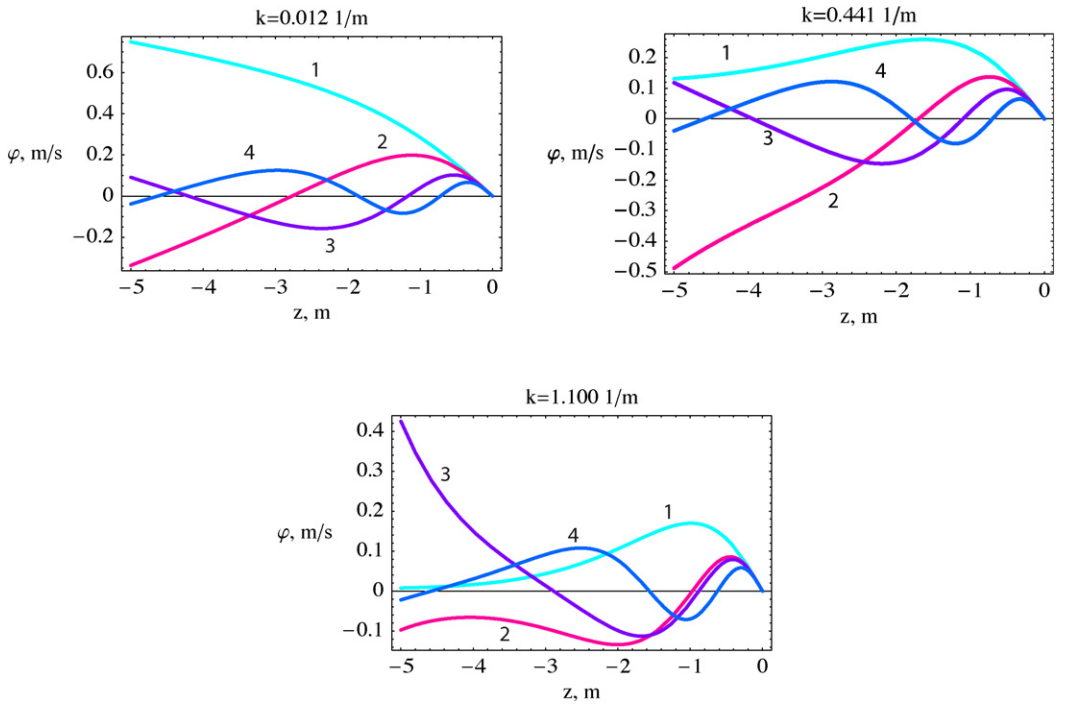

Fig. 9. The first four modal functions for $h = 5$ m, $\gamma = 1$ m^{-1}, $\alpha_a = 0.01$, $\Delta\rho = 0.001$ (the dispersion curves are shown in Fig. 6).

4.3. Barotropic mode

For completeness, we now consider the barotropic mode, and so we must replace the rigid-lid condition at the upper boundary with the (linearised) free-surface boundary conditions,

$$w|_{z=0} = \eta_t, \tag{57}$$

$$p|_{z=0} = g\rho_0(0)\eta \tag{58}$$

where η is the free surface elevation, and the second condition arises by linearisation of the condition that the full pressure field $p_0(z) + p$ is a constant on the free surface $z = \eta$. Then, using (54), in the Boussinesq approximation (i.e., neglecting terms of relative order $O(\sigma)$), and eliminating p from the boundary conditions (57), (58), we get

$$w_{ztt} - g w_{xx}|_{z=0} = 0. \tag{59}$$

For simplicity, we now consider the same setting as in Section 4.1 and look for solutions of (31) in the form of normal modes

$$w = \phi(z)\exp\big[\mathrm{i}(kx - \omega t)\big] + c.c.,$$

supplemented by the boundary condition (59) at the free surface, and the boundary condition that $w|_{z=-H} = 0$ at the rigid bottom. In the following we ignore the effect of compressibility of the mixture and concentrate on the solution of the leading order problem in (36) ($\varepsilon = 0$), using (41). Thus we now find that the dispersion curves for the normal modes are given by the roots of the following equation,

$$\frac{J_\nu(2\sqrt{a})Y_\nu(2\sqrt{a}\,\mathrm{e}^{-\gamma H/2}) - Y_\nu(2\sqrt{a})J_\nu(2\sqrt{a}\,\mathrm{e}^{-\gamma H/2})}{J'_\nu(2\sqrt{a})Y_\nu(2\sqrt{a}\,\mathrm{e}^{-\gamma H/2}) - Y'_\nu(2\sqrt{a})J_\nu(2\sqrt{a}\,\mathrm{e}^{-\gamma H/2})} = \frac{\alpha_a}{\sqrt{a}}, \tag{60}$$

where the prime denotes differentiation with respect to the argument of a function. The corresponding modal functions assume the (non-normalised) form

$$\phi_{0n}(z) = Y_{\nu_n}\big(2\sqrt{a_n}\,\mathrm{e}^{-\gamma H/2}\big)J_{\nu_n}\big(2\sqrt{a_n}\,\mathrm{e}^{\gamma z/2}\big) - J_{\nu_n}\big(2\sqrt{a_n}\,\mathrm{e}^{-\gamma H/2}\big)Y_{\nu_n}\big(2\sqrt{a_n}\,\mathrm{e}^{\gamma z/2}\big) + c.c.$$
$$(n = 1, 2, 3, \ldots). \tag{61}$$

First, let us note that in the limit of a pure homogeneous fluid, i.e. $\alpha_a \to 0$, $N_l = 0$, the dispersion relation (60) yields the well-known dispersion relation for the surface waves:

$$\omega^2 = gk\tanh kH. \tag{62}$$

Indeed, since $N_l = 0$, the parameter $\nu = 2k/\gamma$ is real. We then consider a small value of α_a for fixed values of k and ω; the parameter $a = g\alpha_a k^2/(\gamma\omega^2)$ is also small. Using the standard expansions of Bessel functions in the vicinity of zero, we obtain the following limit

$$\tanh\frac{\gamma\nu H}{2} = \frac{\nu\alpha_a}{2a},$$

which after the substitution of the expressions for ν and a yields (62).

The dispersion curves and modal functions for the baroclinic modes computed in accordance with the dispersion relation (60) and the formula (61) respectively are essentially the same as in the rigid-lid approximation (42) and so are not shown here. However, in contrast to the dispersion relation (42), the new dispersion relation (60) has one additional root, which corresponds to the barotropic mode. The corresponding dispersion curve is shown in Fig. 10, together with the dispersion curve (62) in the homogeneous fluid in the absence of any bubbles (shown by the dashed line). We see that the curves almost coincide. Similarly we find that the modal functions are virtually indistinguishable. Thus, unlike internal waves, bubble distributions (as well as the basic fluid stratification) have virtually no effect on surface waves, as expected.

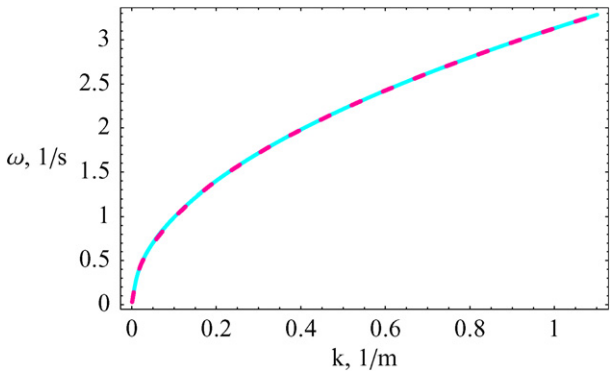

Fig. 10. Dispersion curve for the barotropic mode for $H = 100$ m, $\gamma = 0.5\ \mathrm{m}^{-1}$, $\alpha_a = 0.001$, $N_l = 0.015\ \mathrm{s}^{-1}$ (solid line – in the mixture, dashed line – in the pure homogeneous liquid; the curves coincide).

5. Concluding remarks

In this paper we have considered how the presence of a depth-dependent distribution of bubbles in the fluid waveguide affects the internal normal modes. Restricting attention to the low-frequency case, and then using a quasistatic approximation for the bubbles, has allowed us to formulate an analytical model suitable for polydisperse mixtures (i.e. distributions of bubbles). Consequent asymptotic analysis of our model has shown that, to the leading order in the Boussinesq approximation, the normal modes are described by the usual modal equation, but with an effective buoyancy frequency, which takes account of the near-surface bubble distribution. We then considered two contrasting situations. In the first case the pure fluid has a uniform density stratification, which is then combined with a near-surface, exponentially-decaying void fraction for the bubbles. In the second case, the pure fluid density stratification is modelled by a two-layer fluid. In both these cases we have obtained an explicit description of the normal modes and their corresponding dispersion relations.

Considering typical oceanic parameters, we have shown that bubbles, when present, may change the properties of the oceanic internal waveguide, resulting in the appearance of an additional bubble waveguide in the upper part of the ocean. In particular, even in the absence of any pure fluid density stratification, the density profile due to the bubbles introduces internal wave modes. Note that the corresponding modes may not necessarily be trapped in this thin bubble waveguide, and instead their presence can be felt at a considerable depth. When there is background pure fluid density stratification, we have shown that there are circumstances when there is a potential for a strong interaction between the pure fluid internal wavequide and the upper layer bubble waveguide. In particular, we note that wind-forcing of internal waves may be significantly affected by the presence of an upper bubble layer. Indeed, for those parameter values where the "bubble" modes and the "internal" modes have nearly-intersecting dispersion curves, we would expect that there could be a significant transfer of energy to the "bubble" modes, with consequently less energy penetrating to the deep ocean in the form of "internal" waves. We also would like to note that these bubble modes, when present, could affect the surface signatures of internal waves (a brief outline of current studies on the formation of surface signatures of internal waves can be found, for example, in Apel et al. [23]).

Strictly speaking, the present model has only limited applicability to the description of the *surface* waves in the situation considered in this paper. Indeed, it would be more appropriate to consider large-amplitude breaking surface waves (which are highly non-linear), which inject bubbles into the water (some results in this direction were obtained in a recent paper by Peregrine et al. [24]). Such waves have a large fraction of air in the mixture and foam on the top, and our model is not applicable in this situation. However, we expect our description to be applicable to small amplitude surface waves propagating immediately after the cessation of the breaking of large amplitude surface waves.

Finally, it is appropriate to discuss briefly the physical processes which can maintain a near-stationary depth-dependent bubble distribution. In the oceanic context bubble clouds are repeatedly injected by breaking surface waves, and then evolve under the influence of buoyancy, surface currents, turbulence, dissolution, and bubble break-up. We have taken the view that, acting together, these processes result in the presence of relatively long-lived, quasi-stationary bubble distributions in the upper ocean. The existence of such distributions is supported by the experimental and observational data discussed in the Introduction. Our study suggests that, when looking at typical internal wave time scales, it may be necessary to take account of these bubble distributions. Indeed, density gradients in the ocean are usually small, and it turns out that typical bubble distributions in the upper ocean can produce a density gradient field comparable with that found in the deeper ocean. As we have shown, this can support its own internal wave field, and also significantly modify the internal wave field associated with the density gradient field in the deeper ocean. Nevertheless, the physical processes maintaining the bubble distribution, and the motion of individual bubbles relative to the surrounding fluid are important issues that we would like to address in future work.

Acknowledgements

We thank Ya.V. Kurylev for some clarifying discussions. We thank the London Mathematical Society for their financial support of L.A. Ostrovsky to Loughborough making this collaboration possible. R.H.J. Grimshaw and K.R. Khusnutdinova thank the INTAS grant 06-1000013-9236 for partial support of this research.

References

[1] R.H.J. Grimshaw, K.R. Khusnutdinova, The effect of bubbles on internal waves, J. Phys. Oceanogr. 34 (2004) 477–489.
[2] R.H.J. Grimshaw, K.R. Khusnutdinova, Internal waves in a three-layer bubbly waveguide, Deep-Sea Res. II 51 (2004) 2905–2917.
[3] P.H. LeBlond, L.A. Mysak, Waves in the Ocean, Elsevier, 1978.
[4] A.E. Gill, Atmosphere-Ocean Dynamics, Academic, 1982.
[5] Yu.Z. Miropol'sky, Dynamics of Internal Gravity Waves in The Ocean, Kluwer, 2001.
[6] S.A. Thorpe, On the clouds of bubbles formed by breaking wind-waves in deep water, and their role in air-sea gas transfer, Philos. Trans. R. Soc. Lond. Ser. A 304 (1982) 155–210.
[7] D.M. Farmer, S. Vagle, M. Li, Wave breaking, turbulence and bubble distributions in the ocean surface layer, in: M.L. Banner (Ed.), The Wind-Driven Air–Sea interface, Proceedings, The University of New South Wales, 1999, pp. 187–192.
[8] E.J. Terrill, W.K. Melville, Field measurements of bubble size distributions in the upper mixed layer, in: M.L. Banner (Ed.), The Wind-Driven Air–Sea Interface, Proceedings, The University of New South Wales, 1999, pp. 247–255.
[9] R.I. Nigmatulin, Dynamics of Multiphase Media, vols. 1 & 2, Hemisphere, 1991.
[10] D.M. Farmer, S. Vagle, Wavequide propagation of ambient sound in the ocean-surface bubble layer, J. Acoust. Soc. Am. 86 (1989) 1897–1908.
[11] L. Zedel, D. Farmer, Organized structures in subsurface bubble clouds: Langmuir circulation in the open ocean, J. Geophys. Res. 96 (C5) (1991) 8889–8900.
[12] M.J. Buckingham, Sound speed and void fraction profiles in the sea surface bubble layer, Appl. Acoust. 51 (3) (1997) 225–250.
[13] D.M. Farmer, D.D. Lemon, The influence of bubbles on ambient noise in the ocean at high wind speeds, J. Phys. Oceanogr. 14 (1984) 1762–1778.
[14] S.A. Thorpe, A model of the turbulent diffusion of bubbles below the sea surface, J. Phys. Oceanogr. 14 (1984) 841–853.
[15] Lord Rayleigh, The pressure developed in a liquid on the collapse of a spherical cavity, Philos. Magazine 34 (1917) 94.
[16] S.V. Iordansky, Equations of motion of liquid containing gas bubbles, Zh. Prikl. Mekh. Tekh. Fiz. 3 (1960) 102–110 (in Russian).
[17] B.S. Kogarko, On the model of cavitating liquid, Dokl. AN SSSR 137 (1961) 1331–1333 (in Russian).
[18] L. van Wijngaarden, On the equations of motion for mixtures of liquid and gas bubbles, J. Fluid Mech. 33 (1968) 465–474.
[19] M. Minnaert, On musical air bubbles and the sounds of running water, Philos. Magazine 16 (1933) 235–248.
[20] K.L. Naugolnykh, L.A. Ostrovsky, Nonlinear Wave Processes in Acoustics, Cambridge University Press, 1998.
[21] M. Abramowitz, I.A. Stegun (Eds.), Handbook of Mathematical Functions, Wiley-Interscience, 1972.
[22] C.J. Tranter, Bessel Functions with Some Physical Applications, The English Universities Press, 1968.
[23] J.R. Apel, L.A. Ostrovsky, Y.A. Stepanyants, J.F. Lynch, Internal solitons in the ocean and their effect on underwater sound, J. Acoust. Soc. Amer. 121 (2) (2007) 695–722.
[24] D.H. Peregrine, H. Bredmose, A. McCabe, G. Bullock, C. Obrhai, G. Müller, G. Wolters, Violent water wave impact on walls and the role of air, in: J. MckSmith (Ed.), 29th Internat. Conf. on Coastal Engineering, Proceedings, vol. 4, Lisbon, 2004, World Sci., 2004, pp. 4005–4017.